Available online at www.sciencedirect.com
ScienceDirect
Journal of Nuclear Materials 373 (2008) 299–308
journal of nuclear materials
www.elsevier.com/locate/jnucmat

Development of CAP process for fabrication of ThO_2–UO_2 fuels Part I: Fabrication and densification behaviour

T.R.G. Kutty [a,*], K.B. Khan [a], P.S. Somayajulu [b], A.K. Sengupta [a], J.P. Panakkal [b], Arun Kumar [a], H.S. Kamath [c]

[a] *Radiometallurgy Division, Bhabha Atomic Research Centre, Trombay, Mumbai 400 085, India*
[b] *Advanced Fuel Fabrication Facility, Tarapur, India*
[c] *Nuclear Fuels Group, Bhabha Atomic Research Centre, Trombay, Mumbai 400 085, India*

Received 10 October 2006; accepted 22 June 2007

Abstract

The coated agglomerate pelletization (CAP) process is a novel and innovative technique for the fabrication of (Th, ^{233}U) mixed oxide fuel pellets. This technique is being investigated to fabricate the fuel for the forthcoming Indian Advanced Heavy Water Reactor (AHWR). In the CAP process, ThO_2 is converted to free flowing agglomerate by powder extrusion route. As only ThO_2 is handled to this stage, all the operations are carried out in a normal glove-box facility. Subsequent operations are carried out in a shielded glove-box or hot cell facility using manipulators. In this study, fabrication of ThO_2–4%UO_2 and ThO_2–20%UO_2 (all compositions are in weight percent) pellets was carried out by CAP process. For having these ThO_2–UO_2 pellets, ThO_2 granules and U_3O_8 powders were used as the starting materials. The densification behaviour of the pellets was studied in reducing and oxidizing atmospheres using a high temperature dilatometer. The microstructure was examined by optical microscopy, scanning electron microscopy (SEM) and electron probe microanalysis (EPMA).

PACS: 81.20.Ev; 61.72.−y; 66.30.Fq; 62.20.Fe; 81.70.P

1. Introduction

ThO_2 and UO_2 are identical in crystal structure (fcc CaF_2 type) with close lattice constants of 0.5592 and 0.54704 nm, respectively [1]. Th^{4+} and U^{4+} have similar electronic configurations and their chemical properties are alike. ThO_2 and UO_2 from continuous solid solutions [2,3], i.e. they produce $(Th,U)O_2$ solid solution of the same crystallographic structure at all Th:U ratios [4,5]. ThO_2 solid solution containing around 4%$^{233}UO_2$ (composition in wt%) is the proposed fuel for the forthcoming Advanced Heavy Water Reactor (AHWR) [6]. ThO_2–20%$^{233}UO_2$ is considered as a probable candidate for the fast reactor fuel. The mixed oxide pellets are generally prepared by the conventional powder metallurgy route. Fabrication of $(Th,^{233}U)O_2$ fuel is difficult because it usually contains daughters of ^{232}U (half-life 73.6 years) namely, ^{212}Bi and ^{208}Tl, which emit strong gamma radiations of 0.7–1.8 MeV and 2.6 MeV, respectively. Therefore the fabrication of the thorium fuel requires operations in the shielded glove-boxes to protect the operators from radiation [7–12]. The coated agglomerate pelletization (CAP) process was developed by Bhabha Atomic Research Centre (BARC) to replace the conventional powder metallurgy process that consists of direct blending of $^{233}UO_2$ and ThO_2 powders [13]. The radiation exposure problems can be minimized by quick processing of ^{233}U into finished fuel, as the first decay of ^{232}U has a comparatively longer half-life compared to the remaining daughter products.

The flow sheet of the CAP technique is made of the segmented processes to be performed in the unshielded

* Corresponding author. Fax: +91 22 2550 5151.
E-mail address: tkutty@barc.gov.in (T.R.G. Kutty).

0022-3115/$ - see front matter © 2007 Elsevier B.V. All rights reserved.
doi:10.1016/j.jnucmat.2007.06.010

and shielded facilities on the assumption to use freshly prepared ^{233}U oxide in order to minimize man-rem problem. The main reasons for developing the CAP technique to produce (Th–U)O_2 fuel are [13]:

- to minimize the dusty operations,
- to minimize the number of process steps requiring shielded operation,
- to reduce the man-rem problems since the highly radioactive ^{233}U is confined to only certain steps in the fabrication route.

Thorium fuel cycle is attractive for producing long term nuclear energy with low volume of radiotoxic waste. ^{232}Th is a better fertile material than ^{238}U in thermal reactors since the absorption cross section of ^{232}Th for thermal neutrons is nearly three times that of ^{238}U [14]. In recent years, renewed interest is attached to the thorium cycle because of the following reasons [14]:

(i) the intrinsic and proliferation resistance of thorium fuel cycle due to the presence of ^{232}U,
(ii) better thermo-physical properties and chemical stability of ThO_2, as compared to UO_2,
(iii) lesser long lived minor actinides than those found in the uranium cycle,
(iv) superior plutonium incineration in $(Th, Pu)O_2$ fuel as compared to $(U, Pu)O_2$ and
(v) attractive features of thorium related to accelerated driven system (ADS) and energy amplifier (EA).

Indian nuclear power programme is based on closed nuclear fuel cycle for the efficient utilization of its nuclear resources. India has vast reserves of thorium. The currently known Indian thorium reserves amount to 358 000 GWe-yr of electrical energy, which meet the energy requirements during the next century and beyond that. As mentioned above, the mixed oxide of ThO_2 with around 4%$^{233}UO_2$ (containing about 2–5 ppm of ^{232}U) is proposed fuel for the forthcoming Advanced Heavy Water Reactor (AHWR), which is being developed in India with the specific aim to utilize thorium for power generation. This reactor is of vertical pressure tube type cooled by boiling light water and moderated by heavy water. It incorporates several advanced passive safety features, e.g., heat removal through natural circulation. The reactor has been designed to produce 920 MW(th) at a discharge burn-up of fuel in excess of 24 000 MWd/te [6].

The goal of this work is to develop mixed thorium–uranium dioxide (ThO_2–UO_2) fuel by CAP technique using ThO_2 granules and U_3O_8 powders as the starting material. MOX fuel is generally manufactured under a stringent quality assurance programme. At each step of the fabrication process, quality assurance plans have been established to verify various factors that affect the fuel performance in the reactor. The criteria for adoption of manufacturing process include the acceptable microstructure and the uniform distribution of fissile elements in the pellet matrix [13]. To verify the above points, detailed studies have been carried out on densification and characterization of ThO_2–UO_2 pellets by optical microscopy, scanning electron microscopy (SEM) and electron probe microanalysis (EPMA). So far, however, studies have not been reported on the above process. The results presented here are divided into two parts. Part 1 deals with procedures for fabrication of ThO_2, ThO_2–4%UO_2 and ThO_2–20%UO_2 pellets by CAP process and its densification behaviour. Part 2 deals with characterization and evaluation of thermophysical properties of the pellets prepared by CAP process.

2. CAP process

The flow-sheet of fabrication of $(Th, U)O_2$ pellets by CAP process is given in Fig. 1. In this process, a wide option is possible for the ThO_2 starting material. ThO_2 should be in the form of free flowing agglomerate which can be obtained either by pre-compaction and granulation technique or by extrusion of powders. The ThO_2 microspheres obtained by sol–gel technique can also be used in the CAP process. To make free flowing agglomerates in the extrusion route, the ThO_2 powder is mixed with an organic binder and extruded through perforated rollers. The CAP process is schematically shown in Fig. 2. The extruded ThO_2 paste is converted to agglomerates in a spherodiser. The agglomerates are sieved and subsequently dried to remove the organic binder. As only ThO_2 is handled up to this stage, all these operations are carried out in a normal alpha tight glove-box facility. The operations carried out under shielding are [13]:

(a) coating of ThO_2 agglomerates with desired amount of ^{233}U oxide,
(b) compaction in a multi-station rotary press into green pellets,
(c) sintering in air,
(d) pellet loading and encapsulation into fuel rods.

Preliminary investigation was carried out to find out the optimum ThO_2 agglomerate size. For this purpose ThO_2 agglomerates were made by extrusion route. These agglomerates were segregated into various classes depending upon their size. This was done by sieving them through various mesh sieves, i.e. −20, −30 and −40 meshes. The maximum particle size corresponding to −20, −30 and −40 meshes are 840, 630 and 420 μm, respectively. The agglomerates segregated were mixed with 4%U_3O_8 powder in a planetary ball mill. The surface area of U_3O_8 powder used in this study was 2.15 m^2/g. The mixed powder was then compacted into pellets at 300 MPa pressure, which were then sintered in air at 1450 °C for 8 h. The obtained density of the sintered pellet was found to be in a range of 90–95% T.D. The as-polished microstructure of the sintered pellet made by using −20 mesh granules was

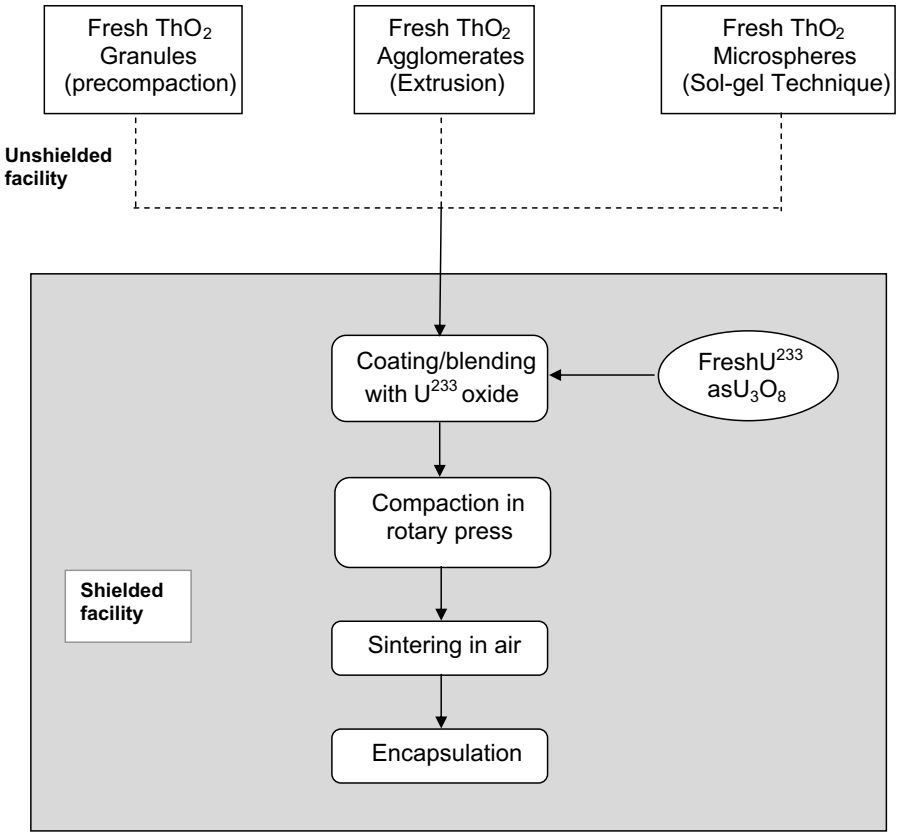

Fig. 1. Flow-sheet for the fabrication of (Th, ^{233}U)O_2 pellets by CAP process.

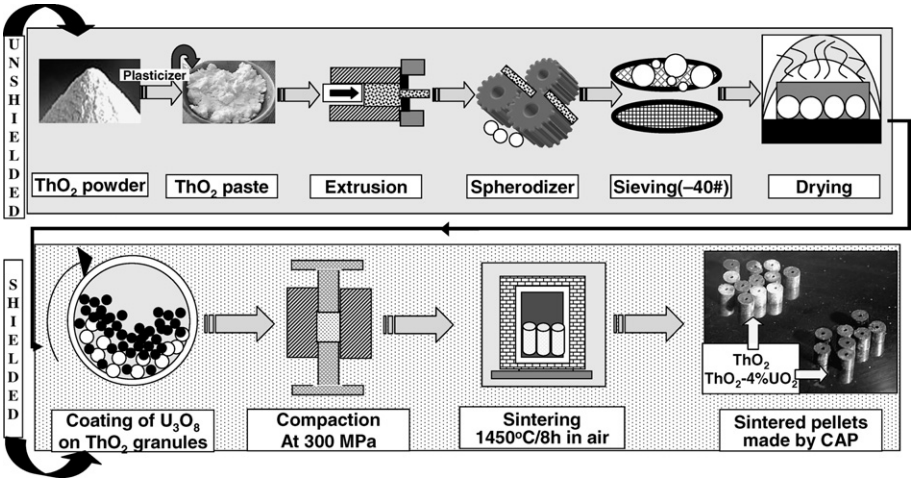

Fig. 2. Schematic diagram of the CAP process for the fabrication of (Th, ^{233}U)O_2 pellets.

unacceptable since it showed delineation of particles at many places. A typical microstructure is shown in Fig. 3(a). This microstructure shows that the identity of the granules is not lost after sintering. The granule is seen as a separate entity with gaps all around which indicate that it has not diffused with other granules properly. The microstructure of −30 mesh sieved granules was better with occasional delineation at fewer places (see Fig. 3(b)). Fig. 3(c) shows as-polished microstructure of a pellet made by using −40 mesh granules. Here, the identity of granules is lost and this pellet shows a satisfactory microstructure with no sign of delineation of granules at any place in the pellet. The above study indicates that −40 mesh ThO_2 granules are best for attaining good microstructure, and therefore all further studies were carried out using the above sized granules.

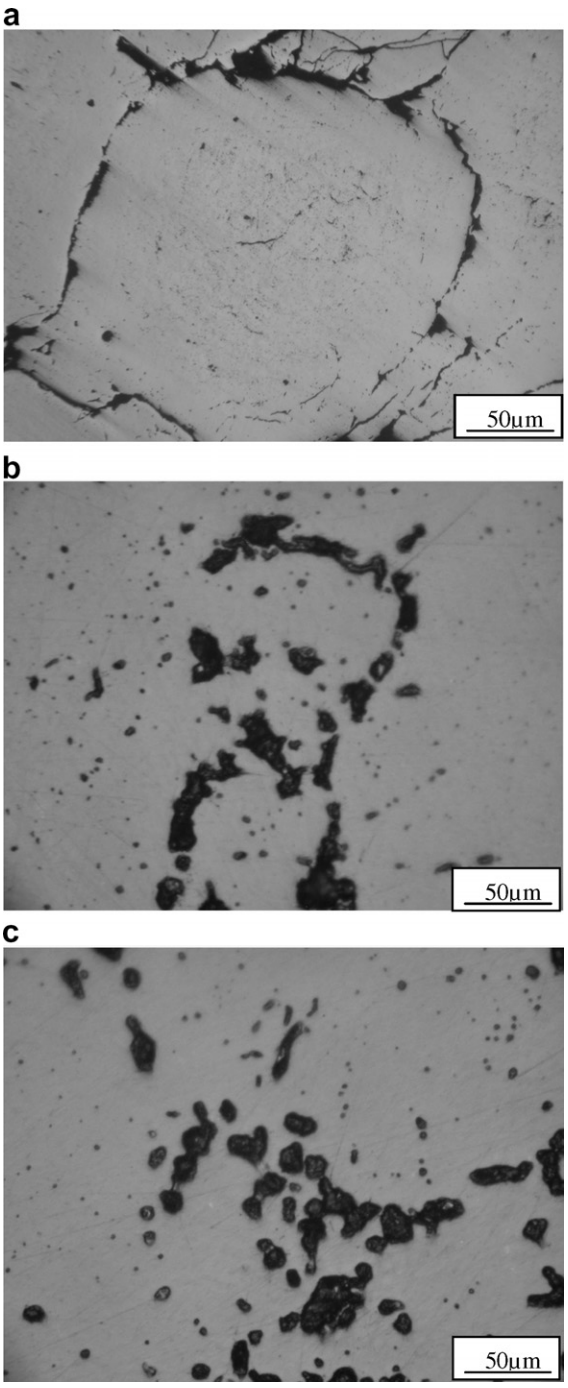

Fig. 3. Typical as-polished microstructures of ThO_2–4%UO_2 pellets obtained using the CAP process with ThO_2 granules of different sizes: (a) with −20 mesh, (b) with −30 mesh and (c) with −40 mesh.

3. Experimental

3.1. Preparation of green compacts

The green pellets of ThO_2–4%UO_2 and ThO_2–20%UO_2 pellets for this study were prepared as described above by the CAP process using ThO_2 granules (−40 mesh) and U_3O_8 powder as the starting material. This work was simulated using natural U instead of ^{233}U. The O/M ratio of the U_3O_8 powder was 2.66. The XRD pattern of the powder indicated that the crystal structure was orthorhombic. The characteristics of the starting ThO_2 and U_3O_8 powders used in this study are given in Table 1. The green density of the compacts was in the range of 62–67% of the theoretical density. To facilitate compaction and to impart handling strength to the green pellets, 1 wt% zinc behenate was added as lubricant/binder during the last 1 h of the mixing/milling procedure. The green pellets were about 12 mm in diameter and around 10 mm in length. A few ThO_2 pellets were also made using the above technique as control samples under identical conditions.

Table 1
Characteristics of ThO_2 and U_3O_8 powders

Property	ThO_2	U_3O_8
Oxygen to metal ratio	2.00	2.66
Apparent density (g/cm^3)	0.70	1.2
Total impurities (ppm)	<1200	<800
Specific surface area (m^2/g)	1.53	2.15
Theoretical density (g/cm^3)	10.00	8.34
Volume relative to ThO_2	1.000	1.273

3.2. Dilatometry

The shrinkage behaviour of ThO_2, ThO_2–4% UO_2 and ThO_2–20% UO_2 pellets was studied using a high temperature dilatometer. The dilatometry was carried out under the following condition:

- force on the sample 0.2 N,
- gas flow 12 l/h,
- heating rate 6 K/min.

Measurements were made by using a Netzsch (model 402E) horizontal dilatometer. The dilatometric data were obtained as the curves of dimension against time and temperature. Here, the sample rests between the push rod and stopper. The change of the length was transmitted through the frictionless push rod to an LVDT transducer. The accuracy of the measurement in length was within ±0.1 μm. A calibrated thermocouple was placed just above the sample to record the sample temperature. The dilatometric experiments were carried out in reducing (Ar–8%H_2) and oxidizing atmospheres (air). The impurity contents of the cover gases used in this study are given in Table 2. The selection of the temperature programme was made by a computer via data acquisition system. The shrinkage of a standard sample (POCO graphite for Ar–8%H_2 atmosphere, alumina for air, NIST) was measured under identical condition in order to correct for the differences in shrinkage between the sample holder and the sample. Table 3 gives the typical impurity contents of a sintered pellet. The density and O/M ratio of the pellets covered in this study are shown in Table 4. From the above table, it can be seen that the O/M ratio of the ThO_2–20%UO_2 pellet after sintering is 2.07. Since ThO_2 cannot form a solid solution with U_3O_8,

Table 2
Impurity contents in the sintering atmospheres (volume ppm)

Sintering atmosphere	Oxygen (vppm)	Moisture (vppm)	CO_2 (vppm)	CO (vppm)	N_2 (vppm)	Oxides of N_2 (vppm)	Hydrocarbon (vppm)
Argon + 8% hydrogen	4	4	1	1	10	1	2
Air	Bal.	10	5	0	Bal.	1	1

Table 3
Metallic impurities in a typical sintered pellet made by CAP process

Element	Impurity (ppm)
Na	14
Al	9
Mg	5
Si	<110
Fe	20
Cr	<1
Co	<5
Ni	<1
Mo	<5
W	<50
Cu	1.0
B	<0.6

Table 4
Density of the sintered ThO_2–UO_2 pellets in the oxidizing and reducing atmospheres

Composition	Density (%T.D.)		O/M ratio	
	Air	Ar–H_2	Air	Ar–H_2
ThO_2	89.8	87.2	2.00	2.00
ThO_2–4%UO_2	94.6	90.5	2.01	2.00
ThO_2–20%UO_2	92.7	85.4	2.07	2.00

the phases expected to be present in this pellet are $(Th, U)O_2$ solid solution and a very small amount of U_3O_8.

3.3. Characterization

The ThO_2, ThO_2–4% UO_2 and ThO_2–20% pellets were characterized by the following techniques:

- thermogravimetry,
- XRD,
- density.

The O/M ratio of the sintered pellet was measured thermogravimetrically using Bahr (Model STA-503) thermal analyzer. The accuracy of the measurement in weight was within ±1 μg. The phase analysis of the ThO_2–20% pellet was carried out using X-ray diffractometry (Diano make, model XRD-8760). The X-ray diffraction patterns of the pellets were obtained by using Cu Kα radiation and graphite monochromator. Accuracy of this equipment is ±5%. The sintered density was determined by means of the Archimedes method.

4. Results

Fig. 4 shows the shrinkage behaviour of ThO_2, ThO_2–4%UO_2 and ThO_2–20%UO_2 pellets in Ar–8%H_2. Here dl/l_0 is plotted against temperature, where lo is the initial length of the pellet in the axial direction and dl is its increment. The corresponding shrinkage rates d(dl/l_0)/dt of the above pellet are shown in Fig. 5. To obtain the value of d(dl/l_0)/dt, the slope of the shrinkage curves, d(dl/l_0)/dT, is multiplied by the heating rate (dT/dt). From Fig. 4, it is evident that the onset of sintering occurs at around 1075 °C for pure ThO_2 while that occurs at about 975 °C

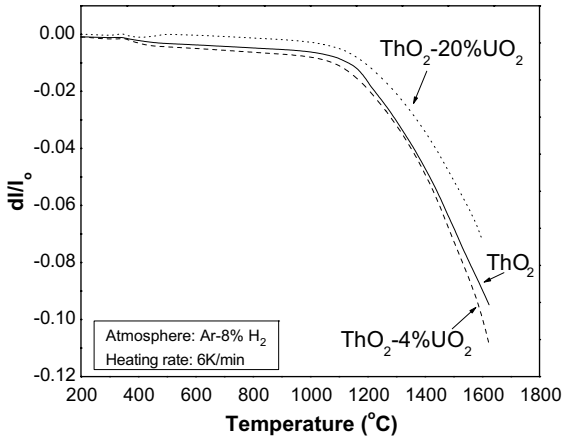

Fig. 4. Shrinkage curves for ThO_2, ThO_2–4%UO_2 and ThO_2–20%UO_2 pellets in Ar–8%H_2. dl is the increment of the length and l_0 is the initial length.

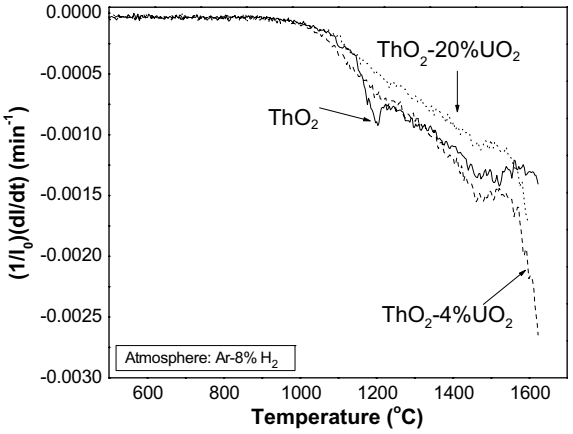

Fig. 5. Shrinkage rate of ThO_2, ThO_2–4%UO_2 and ThO_2–20%UO_2 pellets obtained in Ar–8%H_2 atmosphere plotted against temperature.

for ThO_2–4%UO_2. The onset temperature of shrinkage for ThO_2–20%UO_2 pellet was found to be slightly lower than that of ThO_2–4%UO_2. ThO_2–20%UO_2 showed less shrinkage at all temperatures than ThO_2 and ThO_2–4%UO_2 pellets. The onset temperature of shrinkage was determined from the dilatometric curves by determining the point at which it deviates from its horizontal path. For this, a line is drawn along the linear part of curve. The deviation from linear path is taken as the onset point. Although the difference is small, the onset temperature varies with composition. Fig. 6 shows a plot of shrinkage versus temperature for the above compositions in air. The corresponding shrinkage rates $d(dl/l_0)/dt$ of the above oxides are shown in Fig. 7. The shrinkage behaviour of ThO_2 and ThO_2–4%UO_2 pellets was almost the same in air up to 1100 °C, and above that temperature the shrinkage of ThO_2–4%UO_2 pellet was larger than that of ThO_2. From the above figures (Figs. 6 and 7), it is clear that the onset of shrinkage occurs at around 900 °C in air for ThO_2 and ThO_2–4%UO_2 pellets. The ThO_2–20%UO_2 pellet showed different shrinkage behaviour in air. It showed a gradual shrinkage up to 900 °C followed by an expansion in the temperature range of 900–1100 °C. The onset temperature of shrinkage was about 1175 °C, and the shrinkage behaviour above 1200 °C was not straight forward. The maximum shrinkage rate for the ThO_2–20%UO_2 pellet sintered in air was found to occur at around 1425 °C and that for the ThO_2–4%UO_2 pellet was at around 1520 °C. The maximum shrinkage rate for ThO_2 was found to occur at around 1500 °C. But for the pellets sintered in Ar–8%H_2, no such a maximum were found. Fig. 8 gives intercomparison of shrinkage behaviour of ThO_2–4%UO_2 pellet in reducing (Ar–8%H_2) and oxidizing atmospheres (air). It is evident from the figure that the onset of shrinkage in air occurs at much lower temperature (900 °C) than that in Ar–8%H_2. Fig. 9 compares the shrinkage behaviour of ThO_2–20%UO_2 pellets in air and Ar–8%H_2 atmospheres.

It is possible to compute the shrinkage levels at two different temperatures from Fig. 6 and also know the effect of the addition of UO_2 on the shrinkage at a particular temperature. In air, the shrinkage at 1400 °C was 6% for pure ThO_2 and was 8.5 and 7% for ThO_2–4%UO_2 and ThO_2–

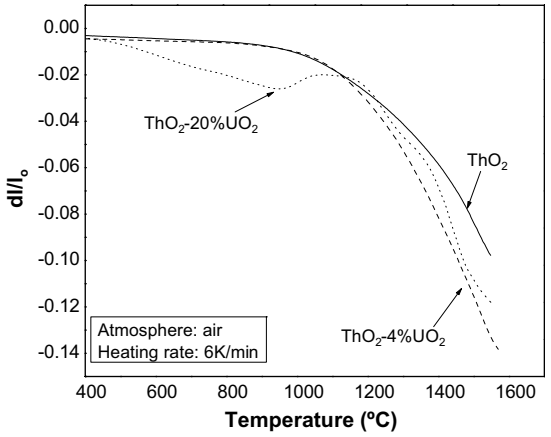

Fig. 6. Shrinkage curves for ThO_2, ThO_2–4%UO_2 and ThO_2–20%UO_2 pellets in air.

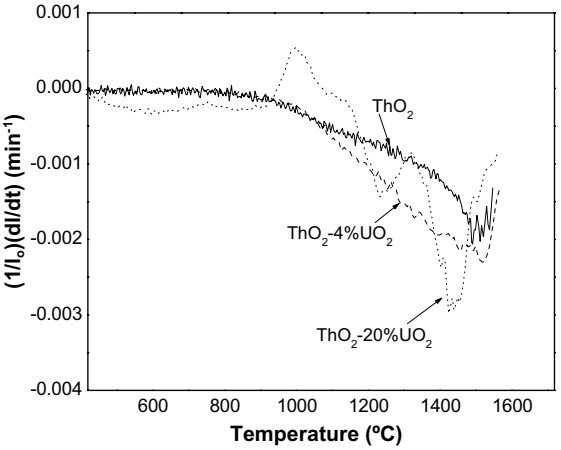

Fig. 7. Shrinkage rate versus temperature curves for ThO_2, ThO_2–4%UO_2 and ThO_2–20%UO_2 pellets obtained in air.

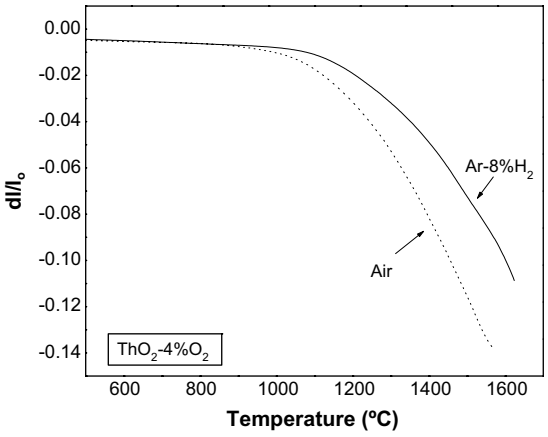

Fig. 8. Effect of atmosphere on the shrinkage behaviour of ThO_2–4%UO_2.

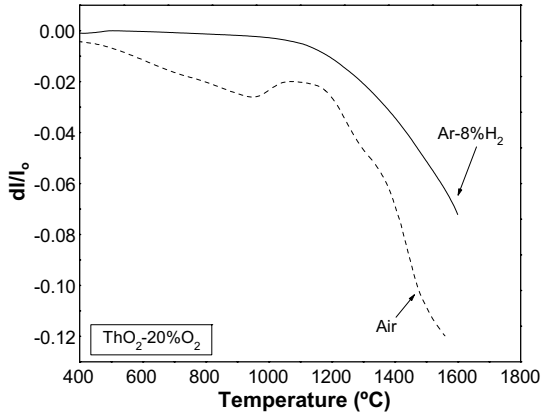

Fig. 9. Comparison of the shrinkage behaviour of ThO_2–20%UO_2 pellet in Ar–8%H_2 and air.

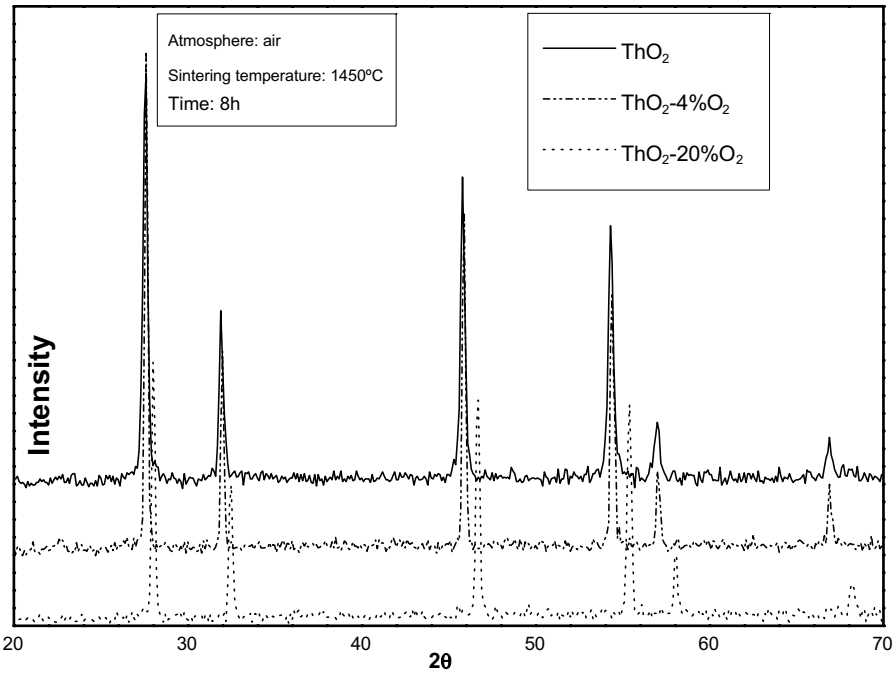

Fig. 10. XRD patterns of ThO_2, ThO_2–4%UO_2 and ThO_2–20%UO_2 sintered pellets.

20%UO_2, respectively. At the same temperature, the shrinkage in Ar–8%H_2 was 4.75% for pure ThO_2 and was 5 and 3.5% for ThO_2–4%UO_2 and ThO_2–20%UO_2, respectively (Fig. 4).

Fig. 10 shows the XRD patterns of ThO_2, ThO_2–4%UO_2 and ThO_2–20%UO_2 pellets. The X-ray diffraction patterns for ThO_2 and ThO_2–4%UO_2 confirm that the compounds are fcc single phased. ThO_2–20%UO_2 should not be single phased, but U_3O_8 peaks cannot be detected in the diffraction pattern possibly because of a small amount. The details of the microstructure are separately discussed in Part II. The significant observations are summarized below:

1. The onset of sintering commences at a temperature which is about 75–150 °C lower in oxidizing atmosphere than that in the reducing atmospheres.
2. In air, the shrinkage behaviour of ThO_2–20%UO_2 pellet was found to be different from that of ThO_2 and ThO_2–4%UO_2 pellets.
3. The maximum shrinkage rate in air was found to occur at around 1520 °C and 1425 °C for ThO_2–4%UO_2 and ThO_2–20%UO_2, respectively.

5. Discussion

As mentioned in Section 1, the CAP process was developed by BARC to replace the conventional powder metallurgy process that directly blends the $^{233}UO_2$ and ThO_2 powders. From the results given in Section 4, it is clear that the high density ThO_2–UO_2 pellets can be fabricated using the CAP process from ThO_2 agglomerates and U_3O_8 powder without the addition of any dopants or sintering aids. The U_3O_8 powder helps to enhance the sintering of ThO_2 compacts, the degree of which depends upon the sintering atmosphere. The exception for this was ThO_2–20%UO_2 pellets which showed entirely different behaviour especially in oxidizing atmosphere: ThO_2–20%UO_2 will be dealt with separately. For ThO_2–4%UO_2 pellets, sintering under oxidizing condition yields a density of around 95% T.D. at around 1550 °C. In the reducing atmosphere, however, a higher temperature of 1600 °C was needed to have the same composition, and its density was only around 90% T.D. (Table 4). These results are very important for the large scale fabrication of ThO_2–UO_2 sintered pellets since the air sintering spares the use of costly cover gas of Ar–H_2. Also costly furnaces with heating elements and sintering boats made of Mo or W are not required [15].

It has been reported that that the solid state solubility of U_3O_8 in ThO_2 is negligible [16,17]. Hund and Niessen [18] studied the entire range of the ThO_2–U_3O_8 system and reported the presence of U_3O_8 phase in addition to the solid solution in the system at higher U_3O_8 contents. However, at lower U_3O_8 content, a single phase structure has been reported. Kutty et al. [19,20] have demonstrated that the addition of small quantities of U_3O_8 to ThO_2 enhances sintering, resulting in formation of high quality ThO_2–UO_2 pellets without the use of conventional dopants such as CaO and Nb_2O_5, which also causes to reduce the impurity level in the pellets. The significance of U_3O_8 addition for enhancing sintering, especially in UO_2, has been discussed by many authors [19–21]. Chevrel et al. [21] indicated that the composition of $UO_{2.25}$ appeared to be the most appropriate for the low temperature sintering. This overall

composition is obtained by the addition of U_3O_8 powder to UO_2. With the above background in mind, we will analyze the shrinkage behaviour of ThO_2–UO_2 compacts made by CAP process in reducing and oxidizing atmospheres covered in this study.

5.1. Ar–8%H_2

Although shrinkage curves of both ThO_2 and ThO_2–4%UO_2 are very close for Ar–8%H_2, the shrinkage of ThO_2–4%UO_2 is a little higher at all temperatures (Fig. 4). The ThO_2–20%UO_2 pellet showed the lowest shrinkage compared to the other two compositions. U_3O_8 present in ThO_2–U_3O_8 compacts is expected to be reduced to UO_2 in Ar–8%H_2 at around 700 °C, giving ThO_2–UO_2 mixture. Since no dopants are added in this compact, sintering will be retarded as ThO_2 and UO_2 are present as perfect stoichiometric compounds [19]. But our study shows the contrary and the sintering has been enhanced for ThO_2–4%UO_2 by the addition of U_3O_8 in Ar–8%H_2 atmosphere. This suggests that U_3O_8 has not been fully reduced to UO_2 at the sintering temperatures. The density of the ThO_2–4%UO_2 pellets obtained in this study in reducing atmosphere is greater than 90% T.D., while that for ThO_2 is only about 87%T.D. for the same atmosphere (Table 4). This clearly shows that the addition of U_3O_8 to ThO_2 has helped in enhancing the sintering.

The onset of sintering for ThO_2–4%UO_2 has been found to occur at around 975 °C, which is less than the onset temperature for sintering for ThO_2. This suggests that U_3O_8 has not been fully reduced to UO_2 at the early stage of sintering. But it might have been reduced to UO_{2+x}. Lay and Carter [22] have evaluated the role of O/U ratio on sintering of uranium dioxide and reported that the uranium diffusion coefficient at the initial stages of sintering of uranium dioxide is dependent on the O/U ratio. They have shown that the uranium diffusion coefficient of uranium dioxide having an O/U ratio of 2.02 is 10^8 times greater than that having an O/U ratio of 2.00. In fact, the diffusion coefficient of uranium, D^U, increases in proportion to x^2. The rate of reduction of U_3O_8 in Ar–8%H_2 atmosphere is surface controlled [22–26]. U_3O_8 will be reduced to $UO_{2.00}$ in Ar–8%H_2 atmosphere even at 700 °C if it is in powder form. In this study, however, we have used green pellets having densities in the range of 62–67% T.D. Hence, the reduction of U_3O_8 to UO_2 could not easily be completed since the gas has to permeate through the dense mass of pellets.

ThO_2–20%UO_2 pellet showed an inferior sintering behaviour in reducing atmosphere in comparison with the other two compositions studied in this work. This result is rather unexpected since ThO_2–20%UO_2 contains a larger amount of U_3O_8, as per the argument given above. This mixed oxide should contain higher concentration of oxygen interstitials which will lead to cause higher shrinkage. Recently Schram [27] has constructed a data base for the oxygen potential of $Th_{1-y}U_yO_{2+x}$ solid solution. The oxygen potential of $Th_{1-y}U_yO_{2+x}$ has been measured by various authors for a wide range of compositions [28–30]. It has shown that the oxygen potential of $Th_{1-y}U_yO_{2+x}$ solid solution decreases with increase in uranium concentration (y) although it increases with the oxygen excess (x). For an O/M ratio of 2.005, Baker et al. [16] have shown that the oxygen potential of ThO_2–20%UO_2 composition at 1200 °C is about 40% lower than that that of ThO_2–5%UO_2. Since ThO_2–20%UO_2 pellet has a lower oxygen potential than ThO_2 and ThO_2–4%UO_2, it may be a factor for its lower shrinkage behaviour. Also the microstructure of the above pellet showed the presence of inhomogeneous microstructure. A typical microstructure of ThO_2–20%UO_2 pellet is shown in Fig. 11. The microstructure consists of large grained areas surrounding the fine grained areas. The large grained areas are highly porous with pore size in the range of 5–10 μm. The highly porous areas are prior U_3O_8 regions. The presence of highly inhomogeneous structure is the another factor for the lower shrinkage behaviour for ThO_2–20%UO_2 pellet in Ar–8%H_2 atmosphere. In fact, the results of this study are in agreement with the work of Song et al. [31]. They have reported that the density of ThO_2–UO_2 mixtures decreases with the U_3O_8 content and decreasing rate is about 2% of T.D. per 10 wt% U_3O_8. They attributed this behaviour to the specific surface area of the U_3O_8 powder which is much lower than the UO_2 powder.

5.2. Air

This study shows that air is better as the atmosphere for sintering of ThO_2–U_3O_8 compacts. As mentioned before, a density of ~95%T.D. was obtained for ThO_2–4%UO_2 pellet in air. In this atmosphere, the ThO_2–20%UO_2 pellet showed higher shrinkage than the ThO_2 pellet in the temperature range of 1250–1550 °C (Fig. 6). It may be the case that U_3O_8 has not been fully reduced to stoichiometric $UO_{2.00}$ on heating in air even at 1550 °C. To confirm this, thermogravimetry for the green powders (consisting of ThO_2 granules and U_3O_8 powder) of ThO_2–4%UO_2 and ThO_2–20%UO_2 has been carried out in air up to 1400 °C.

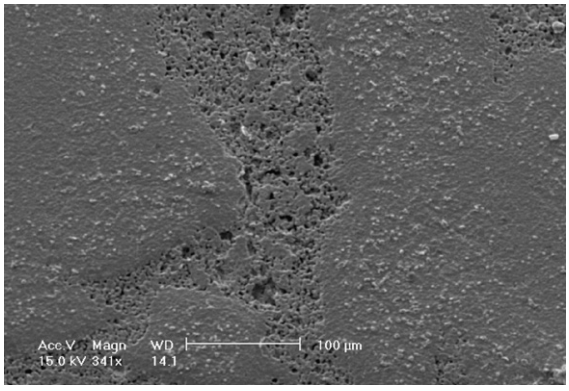

Fig. 11. Microstructure of a ThO_2–20%UO_2 pellet sintered in Ar–8%H_2 showing inhomogeneous microstructure.

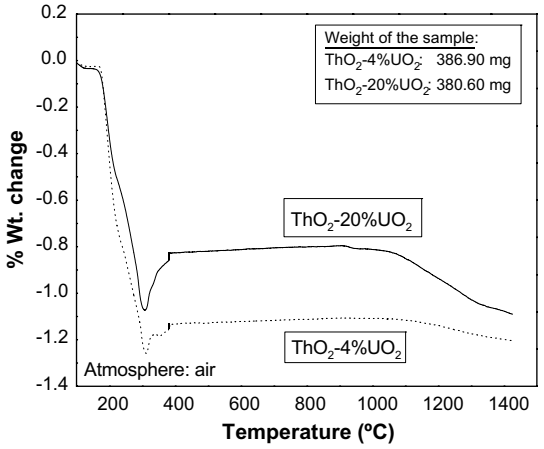

Fig. 12. Thermogravimetric curve showing weight change of ThO_2–4%UO_2 and ThO_2–20%UO_2 powders when heated in air.

The thermograms obtained are given in Fig. 12. The decrease in weight up to 400 °C is due to the evaporation of moisture and burning out of binder. For ThO_2–4%UO_2, there is almost no weight loss up to 1100 °C, and above this temperature a gradual weight decrease is observed. For ThO_2–20%UO_2, there is virtually no weight loss up to 900 °C and above this temperature a dip is seen in the curve, which is followed by gradual decrease in weight up to 1100 °C. Above 1100 °C, the weight loss is steep. However, the weight loss is not complete even at the highest temperature (1400 °C) for both samples, indicating that U_3O_8 has not fully reduced to stoichiometric $UO_{2.00}$.

The increase in the non-stoichiometry by the addition of U_3O_8 to ThO_2 will help in improving the sintering. The decomposition of added U_3O_8 produces a network of fine pores [21,32]. This results in an increase in the total surface area in the sample which helps in enhancing the sintering [33–36].

In the lower temperature range of 400–900°C, the ThO_2–20%UO_2 pellet showed a gradual shrinkage (Fig. 6). But it expanded with increasing temperature in the temperature range of 950–1050 °C. Dilatometric experiment was repeated in air to confirm the above behaviour and good reproducibility was obtained. This expansion caused the formation of surface cracks which is manifested in the shrinkage curve at around 950–1050 °C (Fig. 6). The weight loss observed at 950–1050 °C for ThO_2–20%UO_2 pellet in thermogravimetry was not noticed for ThO_2–4%UO_2 pellet. This is because the amount of U_3O_8 present in the above composition is small and therefore the corresponding weight change was also small.

The expansion observed for ThO_2–20%UO_2 pellet in the temperature range of 950–1050 °C in air was not seen for the same composition pellet in Ar–8%H_2. Let us discuss this point. It has already been mentioned that U_3O_8 can be easily reduced to stoichiometric UO_2 even at a low temperature of 700 °C. Hence U_3O_8 present in ThO_2–20%UO_2 green pellet might have been reduced to UO_{2+x} in Ar–8%H_2 at temperatures well below the temperature at which the above expansion was observed in air. Therefore the expansion was not seen in reducing atmosphere for the above composition.

6. Conclusions

This study has demonstrated that high density ThO_2–UO_2 pellets can be fabricated by CAP route using ThO_2 granules and U_3O_8 powders as the starting materials. The densification behaviour of ThO_2, ThO_2–4%UO_2 and ThO_2–20%UO_2 pellets was evaluated using a high temperature dilatometry in Ar–8%H_2 and in air. The following conclusions are drawn:

(a) In air and Ar–8%H_2 atmospheres, the densification of ThO_2 and ThO_2–4%UO_2 pellets was found to be slightly superior in air. The onset of sintering commences at a temperature which is about 75–150 °C lower in air than that in Ar–8%H_2 atmospheres.
(b) The shrinkage behaviour of ThO_2–20%UO_2 pellet was found to be inferior in Ar–8%H_2.
(c) Thermogravimetric studies carried out in air on ThO_2–4%UO_2 and ThO_2–20%UO_2 granules indicate a continuous decrease in weight until 1400 °C indicating that U_3O_8 is in way to change to stoichiometric UO_2 up to this temperature.
(d) The expansion shown by ThO_2–20%UO_2 pellet in air in the temperature range of 950–1100 °C resulted in the formation of surface cracks.

References

[1] The Chemistry of Actinide and Transactinide Elements, 3rd Ed., vol. 1, Springer, 2006.
[2] K.C. Radford, R.J. Bratton, J. Nucl. Mater. 57 (1975) 287.
[3] E. Slowinski, N. Elliot, Acta Cryst. 5 (1972) 768.
[4] Y. Atlas, M. Eral, H. Tel, J. Nucl. Mater. 249 (1997) 46.
[5] CRC Handbook of Chemistry and Physics, CRC Press, Boca, Raton, Fl, 1984.
[6] A. Kakodkar, in: 46th General Conference of the International Atomic Energy Agency, IAEA, Vienna, 2002.
[7] Hj. Matzke, J. Van Geel, J. Magill, in: Top Fuel '97, vol. I (BNES, London, 1997), p. 4.32.
[8] M.S. Kazimi, M.J. Driscoll, R.G. Ballinger, K.T. Clarno, K.R. Czerwinski, P. Hejzlar, P.J. LaFond, Y. Long, J.E. Meyer, M.P. Reynard, S.P. Schultz, X. Zhao, Proliferation Resistant, Low Cost, Thoria–Urania Fuel for Light Water Reactors, Annual Report, Nuclear Engineering Department Massachusetts Institute of Technology, Cambridge, MA June 1999.
[9] Philip E. MacDonald, Advanced Proliferation Resistant, Lower Cost, Uranium–Thorium Dioxide Fuels for Light Water Reactors, US Department of Energy Nuclear Energy Research Initiative, NERI 99-0153, 1999.
[10] M.S. Kazimi, E.E. Pilat, M.J. Driscoll, Z. Xu, D. Wang, X. Zhao, in: International Conference on: Back-End of the Fuel Cycle: From Research to Solutions, Global 2001, Paris, France, September 2001.
[11] M.S. Kazimi, K.R. Czerwinski, M.J. Driscoll, P. Hejzlar, J.E. Meyer, On the Use of Thorium in Light Water Reactors, MIT-NFC-0016, Nuclear Engineering Department, MIT, April 1999.

[12] Zhao Xianfeng, M.J. Driscoll, M.S. Kazimi, Trans. Am. Nucl. Soc. 80 (1999) 43.
[13] H.S. Kamath, 14th Annual Conference of Indian Nuclear Society, IGCAR, Kalpakkam, December 17–19, 2003.
[14] Thorium Fuel Cycle – Potentials Benefits and Challenges, IAEA-TECDOC-1450, International Atomic Energy Agency, Vienna, 2005, p. 1.
[15] C.R.A. Catlow, A.B. LidiardProc. Symp. Themodynamics of Reactor Materials, vol. II, IAEA, Vienna, 1974, p. 27.
[16] K. Bakker, E.H.P. Cordfunke, R.J.M. Konings, R.P.C. Schram, J. Nucl. Mater. 250 (1997) 1.
[17] R. Paul, C. Keller, J. Nucl. Mater. 41 (1971) 133.
[18] F. Hund, G. Niessen, Z. Elecrochem. 56 (1952) 972.
[19] T.R.G. Kutty, K.B. Khan, P.V. Hegde, A.K. Sengupta, S. Majumdar, H.S. Kamath, Sci. Sintering 35 (2003) 125.
[20] T.R.G. Kutty, P.V. Hegde, K.B. Khan, T. Jarvis, A.K. Sengupta, S. Majumdar, H.S. Kamath, J. Nucl. Mater. 335 (2004) 462.
[21] H. Chevrel, P. Dehaudt, B. Francois, J.F. Baumard, J. Nucl. Mater. 189 (1992) 175.
[22] K.W. Lay, R.E. Carter, J. Nucl. Mater. 30 (1969) 74.
[23] S. Perrin, M. Pijolat, F. Valdivieso, M. Soustelle, in: High Temperature Corrosion and Materials Chemistry, 203rd Meeting of The Electrochemical Society, Paris, April 27–May 3, 2003.
[24] Kun Woo Song, Keon Sik Kim, Youn Ho Jung, J. Nucl. Mater. 277 (2000) 356.
[25] J. Belle, B. Lustman in: Properties of UO_2, Fuel Elements Conference, Paris, TID-7546, 1958, p. 442.
[26] W.R. DeHollander, Hanford Report, HW-46685 (1956).
[27] R.P.C. Schram, J. Nucl. Mater. 344 (2005) 223.
[28] M. Ugajin, J. Nucl. Mater. 110 (1982) 142.
[29] T.B. Lindemer, T.M. Besmann, J. Nucl. Mater. 130 (1985) 473.
[30] T. Matsui, K. Naito, J. Nucl. Mater. 132 (1985) 212.
[31] Kun Woo Song, Keon Sik Kim, Youn Ho Jung, J. Nucl. Mater. 277 (2000) 123.
[32] D. Labroche, O. Dugne, C. Chatillon, J. Nucl. Mater. 312 (2003) 21.
[33] R.J. Ackermann, A.T. Chang, J. Chem. Thermodyn. 5 (1973) 873.
[34] H. Assmann, W. Doerr, M. Peehs, J. Nucl. Mater. 140 (1986) 1.
[35] Kun Woo Song, Keon Sik Kim, Ki Won Kang, Youn Ho Jung, J. Nucl. Mater. 317 (2003) 204.
[36] P. Balakrishna, B.P. Varma, T.S. Krishnan, T.R.R. Mohan, P. Ramakrishnan, J. Nucl. Mater 160 (1988) 88.